

## Supporting information

### A renewable biomass-based lignin film as an effective protective layer to stabilize zinc metal anodes for high-performance zinc-iodine batteries

Ke Wang,<sup>a</sup> Jia-Bo Le,<sup>b</sup> Shao-Jian Zhang,<sup>c</sup> Wen-Feng Ren,<sup>\*,a</sup> Jiang-Meng Yuan,<sup>a</sup>

Ting-Ting Su,<sup>a</sup> Bing-Yu Chi,<sup>a</sup> Chang-You Shao,<sup>a</sup> and Run-Cang Sun<sup>\*,a</sup>

<sup>a</sup>*Liaoning Key Laboratory of Lignocellulose Chemistry and BioMaterials, Liaoning Collaborative Innovation Center for Lignocellulosic Biorefinery, College of Light Industry and Chemical Engineering, Dalian Polytechnic University, Dalian 116034, China*

<sup>b</sup>*Ningbo Institute of Materials Technology and Engineering, Chinese Academy of Sciences, Ningbo 315201, China*

<sup>c</sup>*School of Chemical Engineering & Advanced Materials, The University of Adelaide, Adelaide, SA 5005, Australia*

E-mail address: rcsun3@dlpu.edu.cn, wfren@dlpu.edu.cn.

## Experimental Section

### Electrochemical tests

Electrochemical impedance spectroscopy (EIS) of the cycled bare Zn and Zn@L electrodes was conducted in a frequency range of 100 KHz to 10 mHz with a voltage amplitude of 5 mV. Before EIS measurements, bare Zn and Zn@L symmetric batteries were operated at the current density of 2 mA cm<sup>-2</sup> with the fixed capacity of 2 mAh cm<sup>-2</sup> for different cycles on the battery test system (3001A, Land, China).

The diffusion coefficient was conducted by using Galvanostatic Intermittent Titration Technique (GITT) and calculated based on Eq. as follows (Adv. Funct. Mater. 2019, 29, 1808375):

$$D = \frac{4L^2}{\pi t} \left( \frac{\Delta E_s}{\Delta E_t} \right)^2$$

Where t is the duration of the current pulse, ΔE<sub>s</sub> is the steady-state potential change by the current pulse. ΔE<sub>t</sub> is the potential change of the constant current pulse excluded the iR drop, L is ion diffusion length.

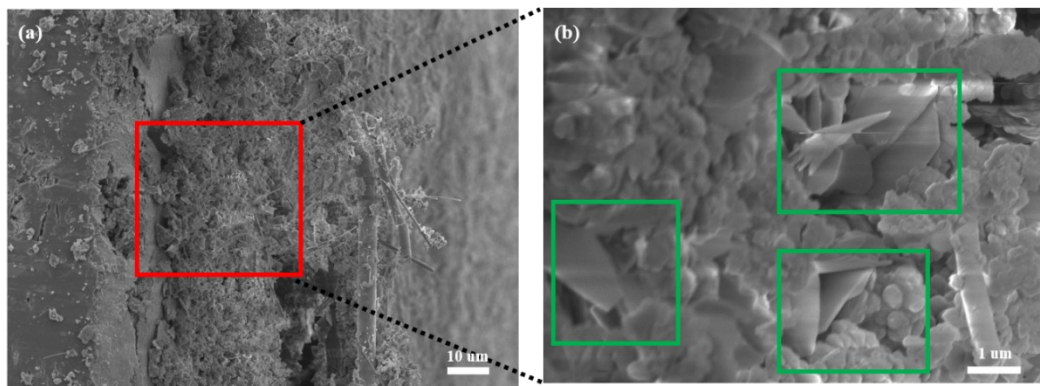


**Figure S1.** The cross-sectional SEM and partial enlarged images of Zn@L electrodes after the deposition of Zn with the capacity of  $2 \text{ mAh cm}^{-2}$ .

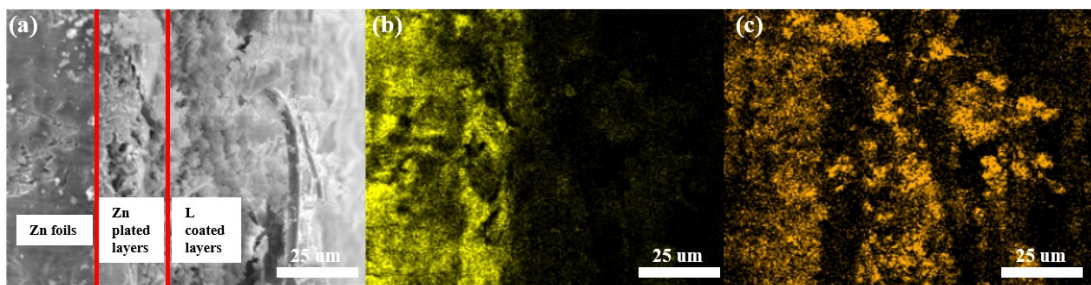


**Figure S2.** The cross-sectional SEM (a) and the corresponding Zn (b) and C (c) element mapping images of Zn@L electrodes after the deposition of Zn with the capacity of 2 mAh cm<sup>-2</sup>.

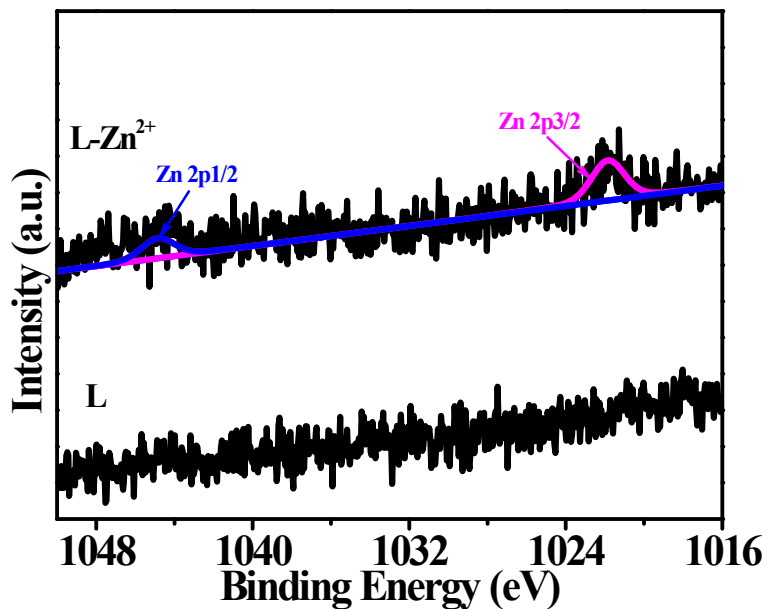


**Figure S3.** XPS spectra of Zn 2p for L powers before and after immersing in 2 M  $\text{ZnSO}_4$  solution for 24 h.

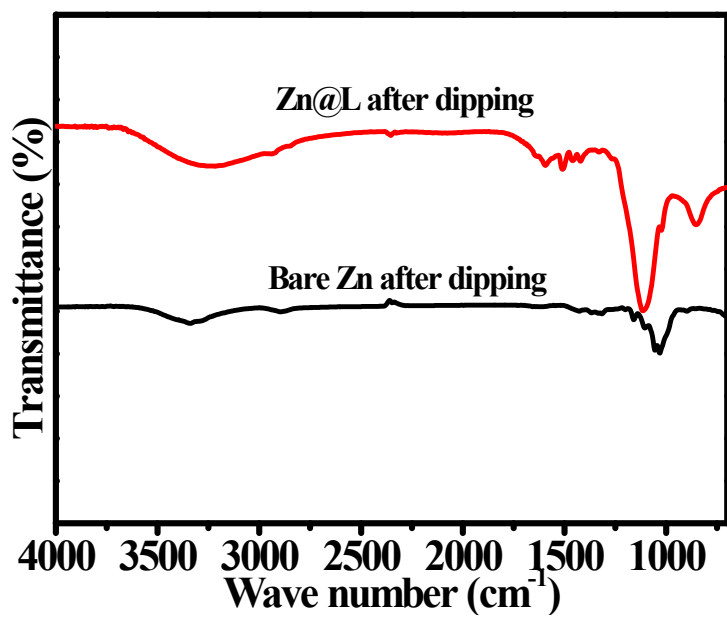


**Figure S4.** FTIR spectra of bare Zn and Zn@L after dipping in electrolyte for 7 days.

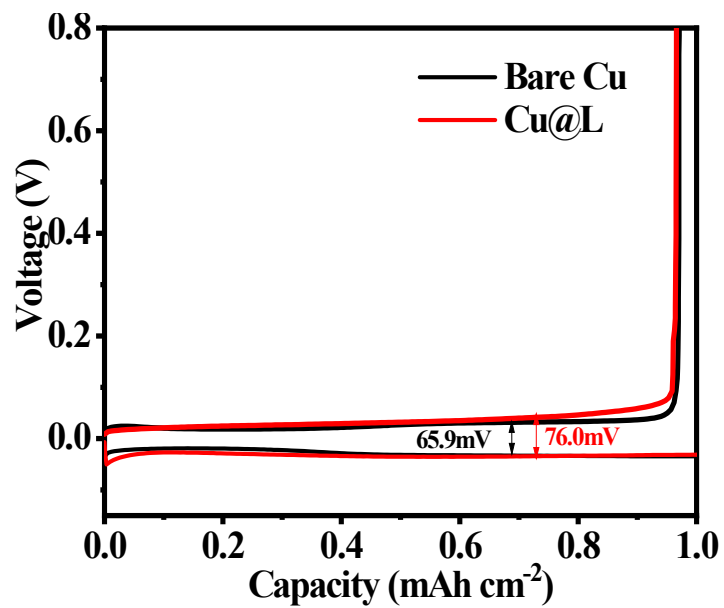


**Figure S5.** The 1<sup>st</sup> charge and discharge curves of bare Cu-Zn and Cu@L-Zn batteries.

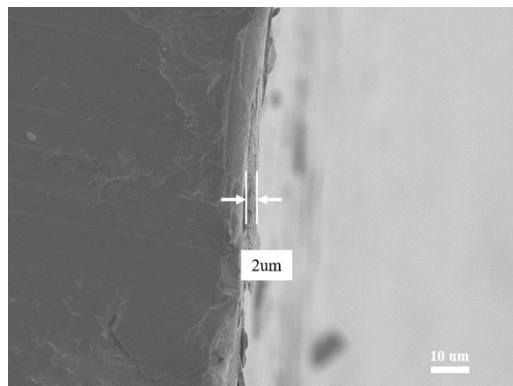


**Figure S6.** The cross-sectional SEM image of thin L coated Zn@L electrodes.

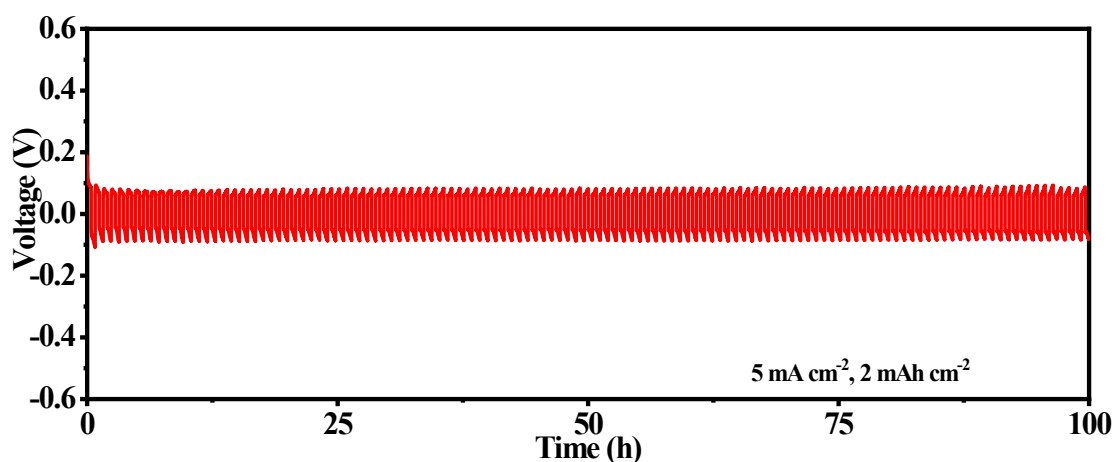


**Figure S7.** The galvanostatic cycling curves of thin L ( $\sim 2 \mu\text{m}$ ) coated Zn@L electrodes at the current density of  $5 \text{ mA cm}^{-2}$  with the fixed capacity of  $2 \text{ mAh cm}^{-2}$ .

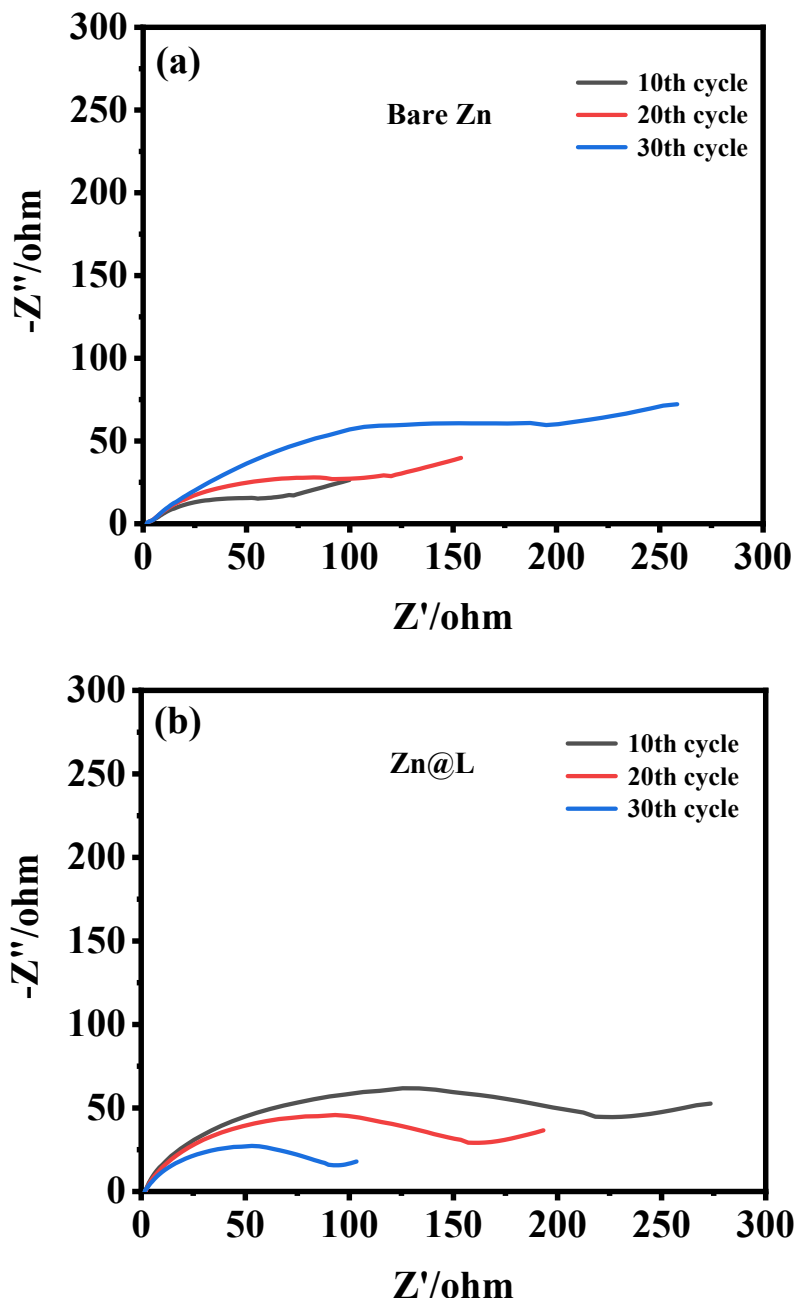


**Figure S8.** EIS spectra of (a) bare Zn and (b) Zn@L symmetric cells at the end of charge process after 10<sup>th</sup>, 20<sup>th</sup>, and 30<sup>th</sup> cycles.

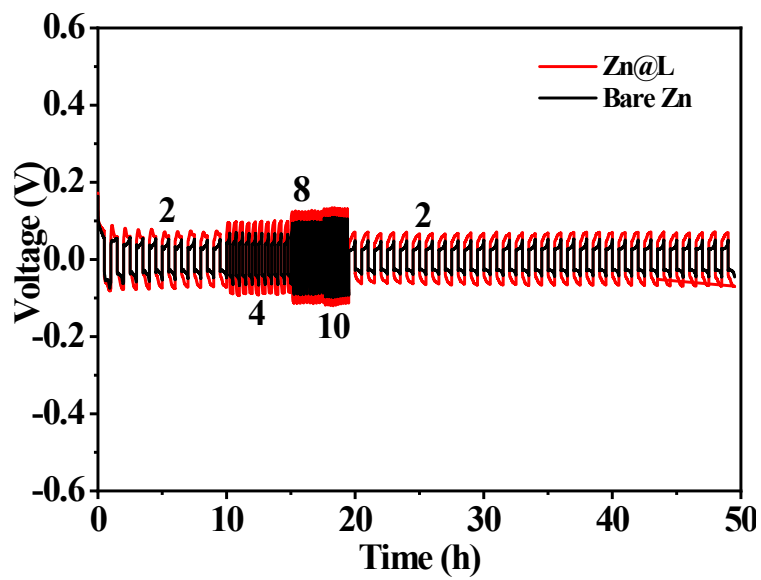


**Figure S9.** Rate performance of bare Zn and Zn@L symmetric cells at the current densities from  $2 \text{ mA cm}^{-2}$  to  $10 \text{ mA cm}^{-2}$  with the capacity limited to  $1 \text{ mAh cm}^{-2}$ .



**Figure S10.** The photograph of Zn-Zn transparent cells for biological microscope devices.

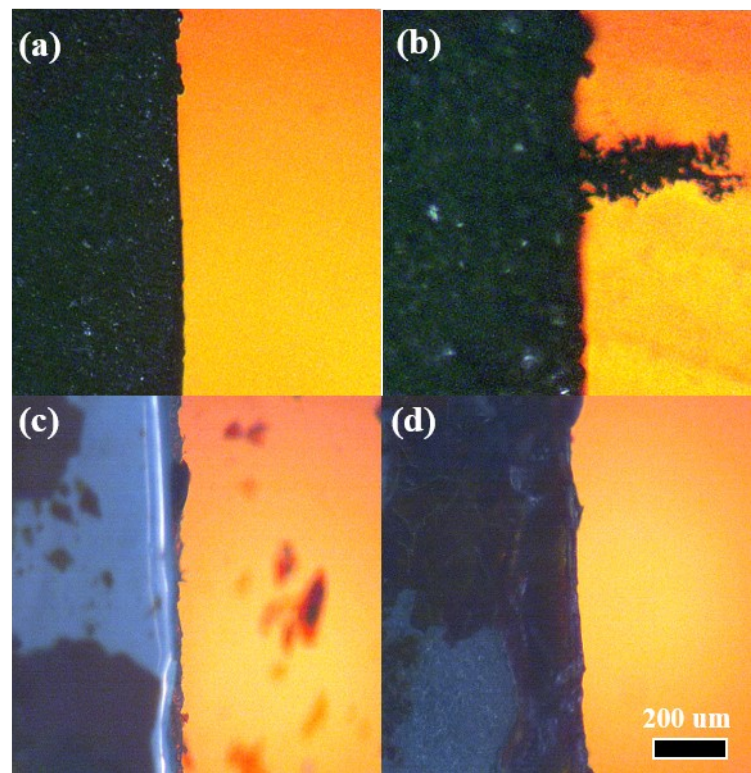


**Figure S11.** Morphology changes of bare Zn (a and b) and Zn@L (c and d) electrodes recorded by optical microscopy via Zn-Zn transparent cells before (a and c) and after (b and d) 5 min plating at 0.02 mA.

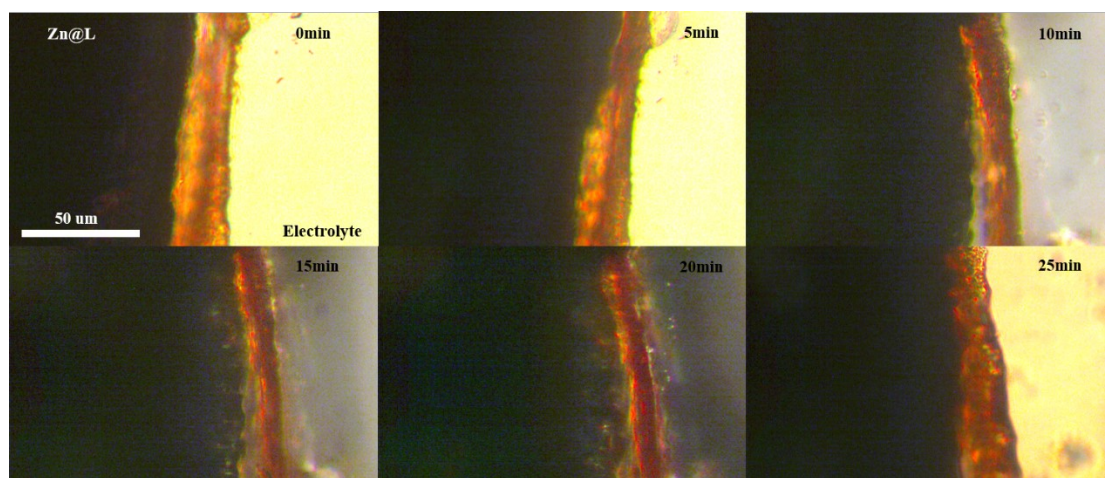


**Figure S12.** Morphology changes of Zn@L electrodes recorded by optical microscopy via the symmetric transparent cells for 0, 5, 10, 15, 20, and 25 min.

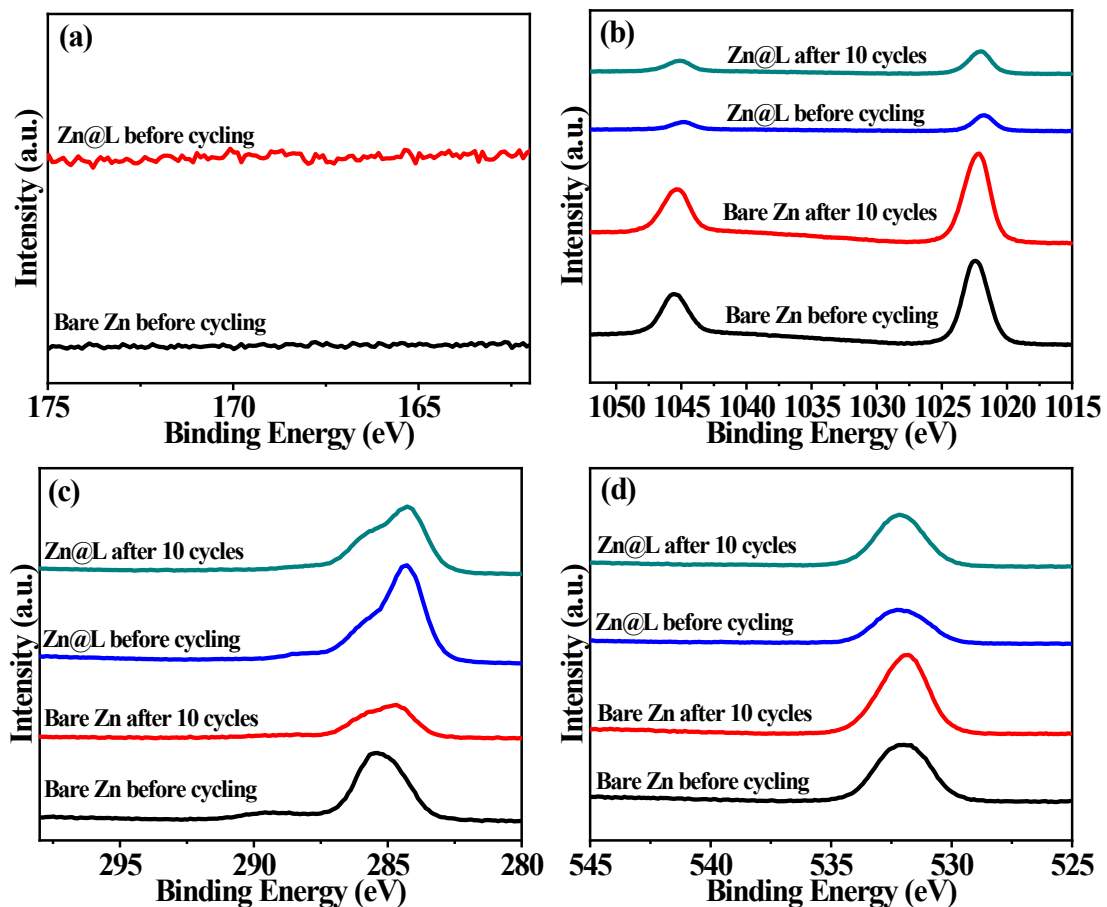


**Figure S13.** XPS spectra of (a) S 2p, (b) Zn 2p, (c) C 1s, and (d) O 1s of bare Zn and Zn@L electrodes before and after 10 cycles.

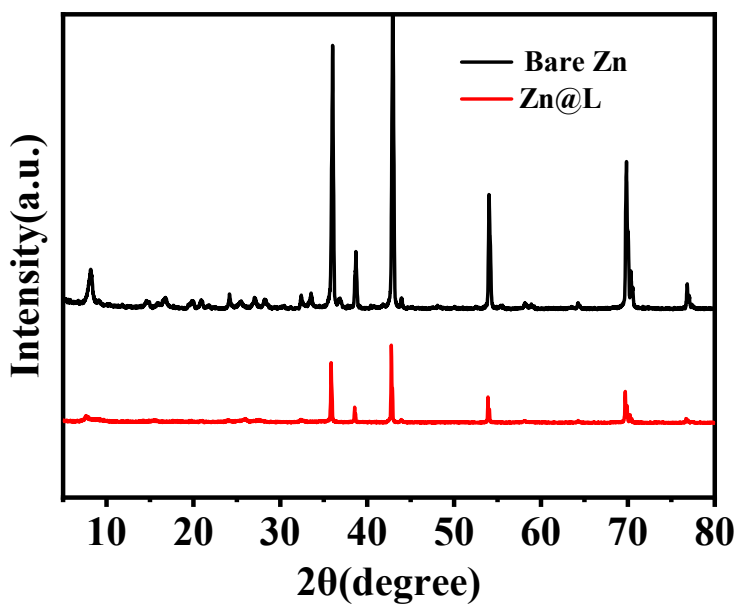


**Figure S14.** XRD patterns of bare Zn and Zn@L electrodes after 10 cycles.

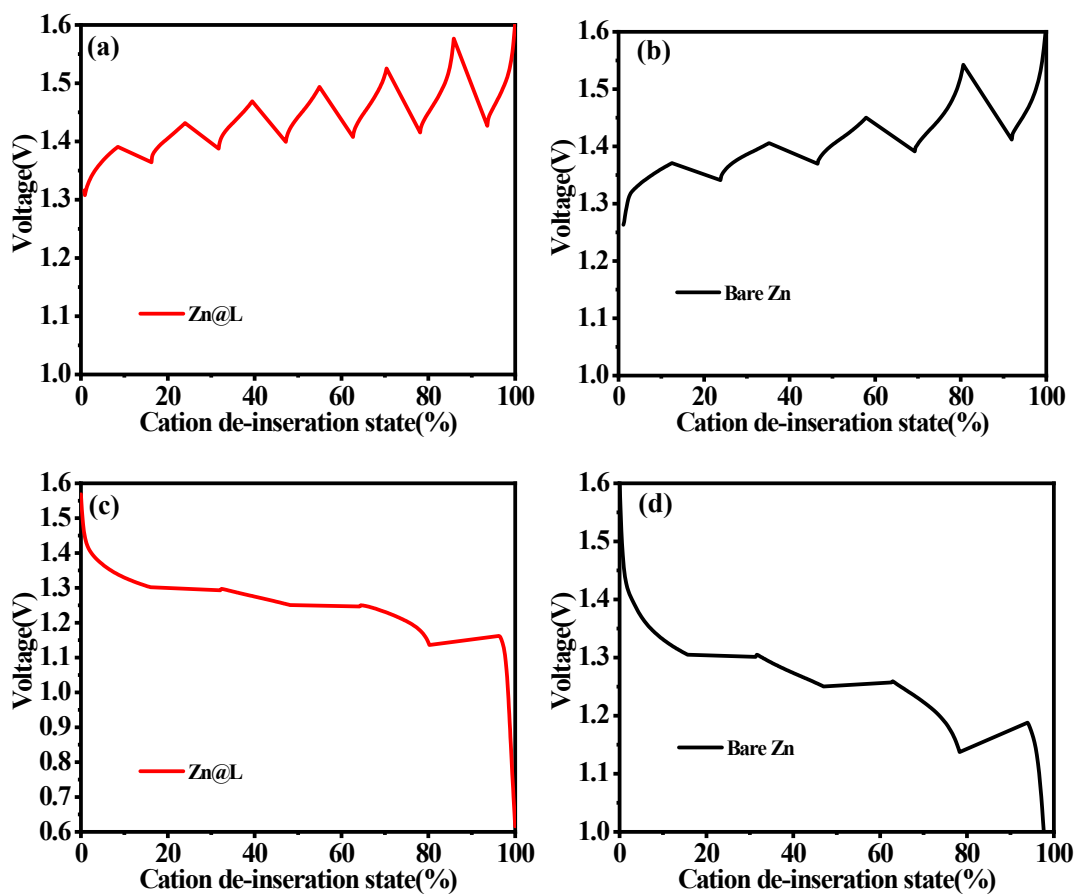


**Figure S15.** GITT curves of full cells with Zn@L (a and c) and bare Zn (b and d)

electrodes.

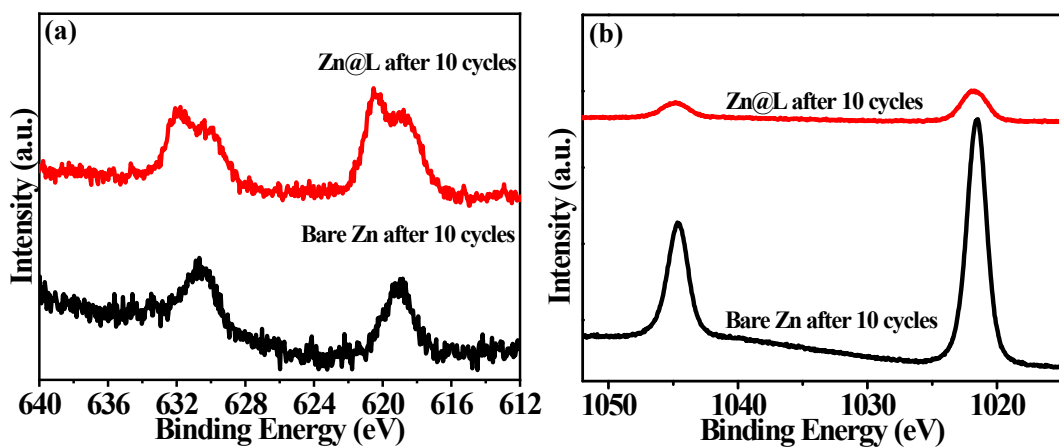


**Figure S16.** XPS spectra of (a) I 3d and (b) Zn 2p of bare Zn and Zn@L electrodes after 10 cycles at the current density of  $1 \text{ A g}^{-1}$ .

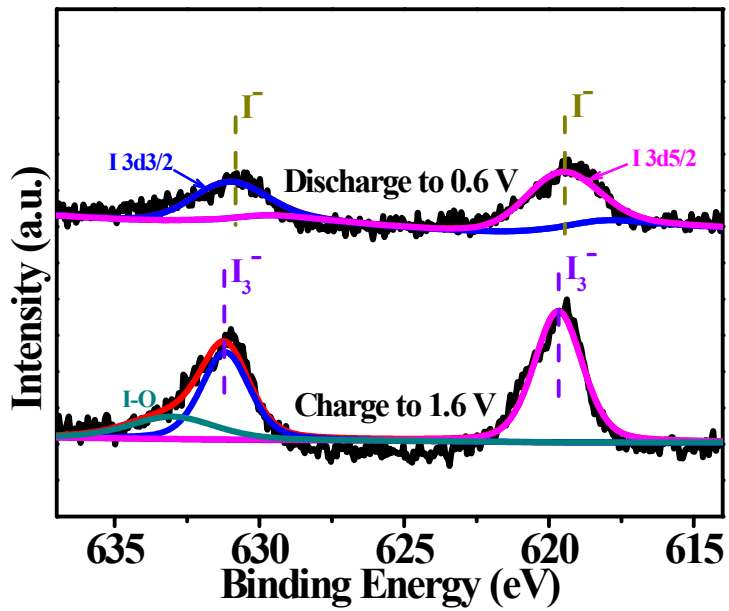


**Figure S17.** XPS spectra of I 3d of I<sub>2</sub>/C cathodes at the charged and discharge state.

**Table S1.** Comparison of corrosion potential shifted values for Zn ion batteries.

Number	Zn metal anodes	Corrosion potential shift	Reference
1	Zn@502 glue	0.013V	[1]
2	Zn@Sb <sub>3</sub> P <sub>2</sub> O <sub>14</sub>	0.004V	[2]
3	Zn	0.004V	[3]
4	Zn@ZnSe	0.004V	[4]
5	Zn@polyamide	0.011V	[5]
6	Zn@L	0.006V	This work

## Reference

1. Z. Cao, X. Zhu, D. Xu, P. Dong, M. O. L. Chee, X. Li, K. Zhu, M. Ye and J. Shen, *Energy Stor. Mater.*, 2021, **36**, 132-138.
2. Y. Zhang, M. Zhu, G. Wang, F. H. Du, F. Yu, K. Wu, M. Wu, S. X. Dou, H. K. Liu and C. Wu, *Small Methods.*, 2021, **5**, 2100650.
3. W. L. Xiong, D. J. Yang, Tuan K.A. Hoang, M. Ahmed, J. Zhi, X. Q. Qiu and P. Chen, *Energy Stor. Mater.*, 2018, **15**, 131-138.
4. X. Yang, C. Li, Z. Sun, S. Yang, Z. Shi, R. Huang, B. Liu, S. Li, Y. Wu, Me. Wang, Y. Su, S. Dou, and J. Sun, *Adv. Mater.*, **33**, 2021, 2105951.
5. Z. Zhao, J. Zhao, Z. Hu, J. Li, J. Li, Y. Zhang, C. Wang and G. Cui, *Energy Environ. Sci.*, 2019, **12**, 1938-1949.

**Table S2.** Comparison of cyclic life of Zn-I<sub>2</sub> batteries.

Cathodes	Anodes	Current density	Capacity	Ref.
I <sub>2</sub> @C-50	Zn	5 A g <sup>-1</sup>	10000 cycles, 90 mA h g <sup>-1</sup>	[1]
I <sub>2</sub> (MOF modified membrane)	Zn	1.92 A g <sup>-1</sup>	6000 cycles, 85.1 mAh g <sup>-1</sup>	[2]
I <sub>2</sub> @C(nanoporous carbon cloth)	Zn	1 A g <sup>-1</sup>	1,500 cycles, 160 mAh·g <sup>-1</sup>	[3]
Co[Co <sub>1/4</sub> Fe <sub>3/4</sub> (CN) <sub>6</sub> ]/I <sub>2</sub>	Zn	4 A g <sup>-1</sup>	2000 cycles, 165.6 mAh g <sup>-1</sup>	[4]
Nb <sub>2</sub> CT <sub>X</sub> /I <sub>2</sub>	Zn	6 A g <sup>-1</sup>	23000 cycles, 140 mAh g <sup>-1</sup>	[5]
I <sub>2</sub> (hydrogel electrolytes)	Zn	2 A g <sup>-1</sup>	2000 cycles, 75.3 mAh g <sup>-1</sup>	[6]
I <sub>2</sub> (acetonitrile electrolyte)	Zn	2 A g <sup>-1</sup>	5,000 cycles, 241.8 mAh g <sup>-1</sup>	[7]
I <sub>2</sub> @C (nitrogen doped carbon)	Zn	2 A g <sup>-1</sup>	10000 cycles, 140 mAh g <sup>-1</sup>	[8]
I <sub>2</sub> @C (microporous carbon)	Zn	0.002 A cm <sup>-2</sup>	200 cycles, 250 mA h g <sup>-1</sup>	[9]
I <sub>2</sub> (solid-state gel catholyte)	Zn	0.2 A g <sup>-1</sup>	500 cycles, 198 mAh g <sup>-1</sup>	[10]
I <sub>2</sub> @C (activated carbon)	Zn (crystal growth controlling)	0.002 A cm <sup>-2</sup>	1000 cycles, 2 mAh cm <sup>-2</sup>	[11]
I <sub>2</sub> @C (activated carbon)	Zn@MOF	4 A g <sup>-1</sup>	20000 cycles, 40 mAh g <sup>-1</sup>	[12]
I <sub>2</sub> /ACF (active carbon fiber cloth)	Zn	0.2 A g <sup>-1</sup>	3000 cycles, 157 mA h g <sup>-1</sup>	[13]
PVP plus KI	Zn	0.02 A cm <sup>-2</sup>	20 cycles, 100 mA h g <sup>-1</sup>	[14]
I <sub>2</sub> /3DGC(3D graphene-like carbons)	Zn	1 A g <sup>-1</sup>	2700 cycles, 200 mA h g <sup>-1</sup>	[15]
I <sub>2</sub>	Zn	0.51 A g <sup>-1</sup>	2000 cycles, 110.9 mA h g <sup>-1</sup>	[16]
I <sub>2</sub>	Zn	0.010 A cm <sup>-2</sup>	2500 cycles, 100% capacity retention	[17]
I <sub>2</sub>	Zn	0.010 A cm <sup>-2</sup>	40 cycles, 123 mA h g <sup>-1</sup>	[18]
I <sub>2</sub> /I <sub>3</sub> <sup>-</sup>	Zn@C	0.2 A g <sup>-1</sup>	500 cycles, 60 mA h g <sup>-1</sup>	[19]
<b>I<sub>2</sub>/C (KB carbon black)</b>	<b>Zn@L</b>	<b>6 A g<sup>-1</sup></b>	<b>35000 cycles, 86.7 mA h g<sup>-1</sup></b>	<b>This work</b>

## Reference

1. W. Li, K. Wang and K. Jiang, *J. Mater. Chem. A.*, 2020, **08**, 1-26.
2. H. Yang, Y. Qiao, Z. Chang, H. Deng, P. He and H. Zhou, *Adv. Mater.*, 2020, **32**, 2004240.
3. C. Bai, F. Cai, L. Wang, S. Guo, X. Liu and Z. Yuan, *Nano Res.*, 2018, **11**, 3548-3554.
4. L. Ma, Y. Ying, S. Chen, Z. Huang, X. Li, H. Huang and C. Zhi, *Angew. Chem. Int. Ed.*, 2021, **60**, 3791-3798.

5. X. Li, N. Li, Z. Huang, Z. Chen, G. Liang, Q. Yang, M. Li, Y. Zhao, L. Ma, B. Dong, Q. Huang, J. Fan and C. Zhi, *Adv. Mater.*, 2021, **33**, 2006897.
6. W. Shang, J. Zhu, Y. Liu, L. Kang, S. Liu, B. Huang, J. Song, X. Li, F. Jiang, W. Du, Y. Gao and H. Luo, *ACS Appl. Mater.*, 2021, **13**, 24756-24764.
7. C. Song, Z. Gong, C. Bai, F. Cai, Z. Yuan and X. Liu, *Nano Res.*, 2021, 1-8.
8. D. Yu, A. Kumar, T. A. Nguyen, M. T. Nazir and G. Yasin, *ACS Sustain. Chem. Eng.*, 2020, **8**, 13769-13776.
9. Y. Li, L. Liu, H. Li, F. Cheng and J. Chen, *ChemComm.*, 2018, **54**, 6792-6795.
10. K. K. Sonigara, J. Zhao, H. K. Machhi, G. Cui and S. S. Soni, *Adv. Energy Mater.*, 2020, **10**, 2001997.
11. S. Jin, D. Zhang, A. Sharma, Q. Zhao, Y. Shao, P. Chen, J. Zheng, J. Yin, Y. Deng, P. Biswal and L. A. Archer, *Small.*, 2021, **17**, 2101798.
12. Z. Wang, J. Huang, Z. Guo, X. Dong, Y. Liu, Y. Wang and Y. Xia, *Joule.*, 2019, **3**, 1289-1300.
13. H. Pan, B. Li, D. Mei, Z. Nie, Y. Shao, G. Li, X. S. Li, K. S. Han, K. T. Mueller, V. Sprenkle and J. Liu, *ACS Energy Lett.*, 2017, **2**, 2674-2680.
14. J. Yang, Y. Song, Q. Liu and A. Tang, *J. Mater. Chem. A.*, 2021, **9**, 16093-16098.
15. H. Park, R. K. Bera and R. Ryoo, *Adv. Energy Sustainability Res.*, 2021, **2**, 2100076.
16. J. Wang, H. Qiu, Z. Zhao, Y. Zhang, J. Zhao, Y. Ma, J. Li, M. Xing, G. Li and G. Cui, *Chem Res Chin Univ.*, 2021, **37**, 328-334.
17. M. Mousavi, G. Jiang, J. Zhang, A. G. Kashkooli, H. Dou, C. J. Silva, Z. P. Cano, Y. Niu, A. Yu and Z. Chen, *Energy Stor. Mater.*, 2020, **32**, 465-476.

18. Z. Pei, Z. Zhu, D. Sun, J. Cai, A. Mosallanezhad, M. Chen and G. Wang, *Mater. Res. Bull.*, 2021, **141**, 111347.
19. K. Lu, H. Zhang, B. Song, W. Pan, H. Ma and J. Zhang, *Electrochim. Acta*, 2019, **296**, 755-761.